METROLOGY AND MEASUREMENT SYSTEMS
VOL. XIV, NUMBER 4 (2007)

JERZY HOJA, GRZEGORZ LENTKA

Gdansk University of Technology
Faculty of Electronics Telecommunications and Informatics, Poland
e-mail: hoja@eti.pg.gda.pl

NEW CONCEPT OF A MEASUREMENT PROBE FOR HIGH IMPEDANCE SPECTROSCOPY

The paper presents a new measurement probe working as the input circuit for a high impedance spectroscopy analyzer. The probe allows to measure impedance in the range of $100\ \Omega < |Z_x| < 100\ G\Omega$. The probe extracts two signals proportional to current through and voltage across the measured impedance in a wide frequency range from 100 μHz to 1 MHz. By the use of a current-to-voltage converter the influence of capacitance of the shielded cables connecting the object under measurement on the result of the measurement is kept as low as possible. An analysis of the probe has been performed taking into account most important parameters influencing the measurement accuracy: parasitic capacitance and real-life parameters of operational amplifiers in use. The formula for calculation of the modulus and argument of the measured impedance has been developed taking into account the correction for real-life parameters of the probe. This allows to decrease the maximal measurement errors of the impedance modulus to ca. 1% and of the impedance argument to 2°, respectively, in the whole range of measurement frequencies.

Keywords: impedance spectroscopy, high impedance measurement

1. INTRODUCTION

For many years, impedance spectroscopy (IS) is one of basic research methods for technical objects which can be modelled by an equivalent electrical circuit. IS is one of the most interesting methods for the characterization of dielectric materials and is widely used in such different areas like electrochemistry [1], ceramic engineering [2], geology [3], buildings [4] or medicine and biology [5]. The measurement procedure of IS consists of two phases. At first, a measurement phase is performed, when the object impedance Z_m is measured as a function of the measurement signal frequency. Next, an analysis phase allows the identification of parameters of RC elements of the equivalent circuit on the basis of the impedance spectrum $Z_m(f)$.

IS is very important in the case of diagnostics of anticorrosion coatings performed either in the laboratory on test samples or on the objects directly in the field (e.g. on bridges, pipelines etc.) [6, 7]. Modern coatings, which are achieving very high impedances $Z_m > 1\ G\Omega$, have forced the need to develop new input circuit solutions

of IS analyzers. In order to identify the parameters of tested coatings, it is necessary to measure impedance in a wide frequency range starting from very low frequencies of the order of 100 μHz up to 1 MHz.

Taking into account the above conditions and the existing need of portable spectroscopy instrumentation, the authors have developed an analyzer for high impedance spectroscopy of anticorrosion coatings. The accuracy of the analyzer is dependent on input circuitry as well as on the method of determining the orthogonal parts of measurement signals. The estimation of the accuracy of the complete measurement path is complicated and very wide, so the paper is focused on input circuitry the influence of which on the measurement error is the highest in case of high impedances measurement (up to 100 GΩ).

The paper presents a new circuit solution of the input circuitry of a high impedance analyzer. The form of the input probe has been selected which allows to keep the influence of parasitic capacitances on accuracy of impedance measurement as low as possible. Limitations will be presented due to real parameters of the probe and their influence on the impedance measurement accuracy. The performed analysis allows to define analytically the output signals of the probe taking into account real parameters of the probe components. This led to estimate the equation which corrects the measurement result. It was implemented in the realized analyzer and has increased the accuracy and maximal frequency of impedance measurement.

2. THE ACHITECTURE OF THE ANALYZER

The presented requirements concerning high impedance measurements at very low frequencies have forced the use of solutions which are not present in conventional instrumentation for impedance measurement. This applies especially to the phase-sensitive detection technique and input circuitry.

- The developed analyzer uses a phase-sensitive detector based on Discrete Fourier Transform (DFT) to determine orthogonal parts (Re $(\cdot)$ and Im $(\cdot)$) of measurement signals on the basis of collected samples of each signal. The use of a digital signal processing technique allows to determine the orthogonal parts at very low frequencies starting from 100 μHz.
- The need of high impedance measurements forced the necessity of shifting the input circuitry from the analyzer's main unit to the external measurement probe. It allows to shortly connect the object under measurement with the input circuitry thus minimizing the influence of parasitic capacitancies on impedance Z_x.

The authors have built an analyzer according to the presented concept. The block diagram of the analyzer is presented in Fig. 1.

The object under measurement is connected to the measurement probe to which signal u_g is applied. The probe extracts two signals proportional to current $u_i \sim i_x$ through and to voltage $u_u \sim u_x$ across the unknown impedance Z_x (these signals allow to determine

impedance on the basis of definition). The signals are sampled and quantised by AD converters located in the main unit of the analyzer. On the basis of two sets of samples of voltages u_i and u_u collected in RAM memories, orthogonal parts of measurement signals U_u and U_i are determined using the DFT transform. In order to simplify calculations a CPLD programmable circuit has been used assuring synchronous generation of signal u_g (strobing DA converter) and sampling of measurement signals by AD converters. The calculations are made by DSP at the end of each measurement cycle. The DSP also calculates the modulus and phase of the measured impedance on the basis of the following formula:

$$|Z_m| = 10\left|\frac{U_u}{U_i}\right|R_R, \qquad \varphi_{Z_m} = \arg\left(\frac{U_u}{U_i}\right), \tag{1}$$

where: R_R – reference range resistor, which is used to convert current i_x to voltage u_i in the probe.

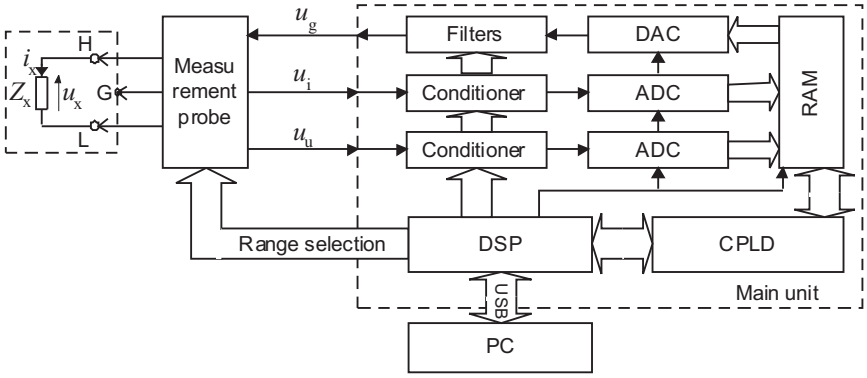

Fig. 1. Block diagram of the analyzer for high impedance spectroscopy.

Figure 2 presents a schematic diagram of the probe. This is a 3-terminal input circuit (H, L, G) realized on the basis of a current-to-voltage converter (amplifier A1), which allows to extract a signal u_i proportional to i_x. The use of the current-to-voltage converter and ground terminal G permits elimination of the influence of parasitic capacitance between the wire connecting the L terminal and the shielding of the object under measurement (shielding of high impedance objects is necessary to eliminate noise entering mainly through power lines). The obtained benefit results from forcing almost zero voltage between terminals L and G by connecting them to the inputs of amplifier A1. There is no current flow between terminal L and G, and the parasitic capacitance appearing between these terminals can be treated as a virtual open circuit. To assure a negligibly low voltage between inputs "–" and "+" of amplifier A1 it is necessary to keep the gain of A1 in the range $-0.01 < k_{A1} \leq -0.1$. Because of this, to achieve a wide range of measured impedance Z_x (current i_x changes from

10 pA ÷ 10 mA), range resistors R_R (1 GΩ, 100 MΩ, 10 MΩ, ... 100 Ω) have been used. They are switched by miniature reed relays.

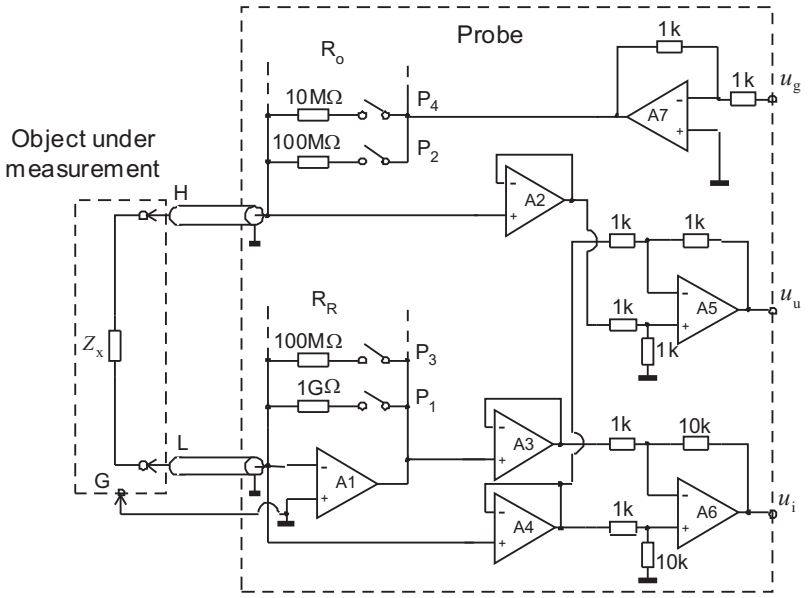

Fig. 2. Schematic diagram of the measurement probe.

When changing the measurement range, resistance R_o is switched simultaneously at the output of amplifier A7, which is the source of the signal applied to Z_x. Resistor R_o ($R_o = 0.1R_R$) limits the current flowing through the current-to-voltage converter in case of a short across Z_x. Because the gain of amplifier A1 is not greater than 0.1, the signal from the current-to-voltage converter is additionally amplified x10 by amplifier A6. Thus the amplitude of signal u_i is comparable with voltage u_u. The voltage u_u is taken from the measured impedance Z_x via voltage followers A2 and A4 and differential amplifier A5.

3. AN ANALYSIS OF THE HIGH IMPEDANCE PROBE

In order to analyze the influence of real-life parameters of operational amplifiers and parasitic capacitances on extracted signals u_i and u_u the probe circuit presented in Fig. 2 was modeled using Spice (Fig. 3) and Matlab (Fig. 4. and 5). The simulations have been made taking into account consecutively the DC and AC parameters of the operational amplifiers and capacitances of the cables connecting the impedance Z_x and parasitic capacitances connected in parallel to range resistors R_R.

3.1. The DC and AC parameters of operational amplifiers

Due to the maximal value of measured impedance $|Z_x|$ = 100 GΩ, operational amplifiers to be used in the input circuitry must have low input currents (on the level of pA) and high differential and common input impedance (Z_d, Z_c) assuming possibly wide frequency bandwidth. The presented constraints cannot be fulfilled, because there are no amplifiers with good parameters for DC and AC at the same time. As a compromise, OPA627 amplifiers have been used with input currents not exceeding 1–2 pA (at 20°C), and Z_c and Z_d impedances are determined by resistances $R_c = R_d$ = 10 TΩ connected in parallel with capacitances C_c = 7 pF, C_d = 8 pF while the GBW = 16 MHz.

In order to evaluate the influence of temperature in the range of −20°C to +70°C on the DC offset of signals u_i and u_u, simulations have been performed for each range resistor (Fig. 3). The worst situation exists in the range R_R = 1 GΩ, because the DC voltage changes from −2 mV to −22 mV for the voltage signal and from 100 mV to 4.6 V for the current signal. In the realized analyzer, the measurement paths for both signals contain offset compensation circuits in the range of ±4 V, so at the highest range the maximum operating temperature should not exceed 60°C. For the range resistor by one order smaller, R_R = 100 MΩ, the maximal value of the DC offset decreases significantly, for u_u down to −2.5 mV, and for u_i down to 0.5 V respectively. For the lower ranges the DC offset is on the level which does not imply a compensation procedure and does not affect the AD converters.

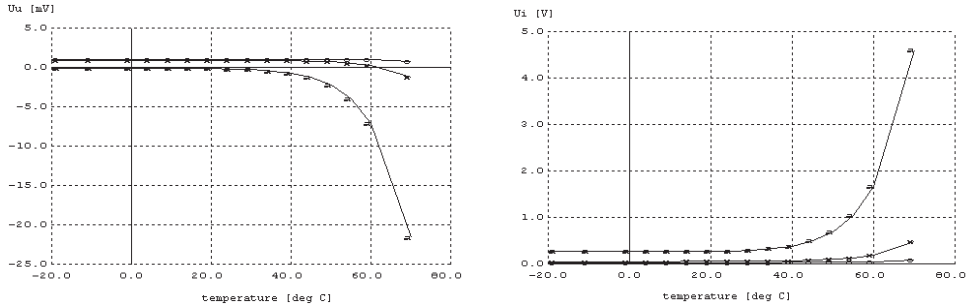

Fig. 3. DC offsets in voltage and current measurement paths for different range resistors: o – R_R = 10 MΩ, x – R_R = 100 MΩ, a – R_R = 1 GΩ.

The analysis of the influence of AC parameters of amplifiers (A_u, ω_{3dB}) on the impedance measurement error has been performed in the high measurement frequency range (> 10 kHz) where their influence is strongest. During the simulation the impedance measurement was analyzed, because in this way the ratio of signals from both paths is determined and noticeable reduction of gain and phase errors exists. It results from similar configuration of both paths. In case of the use of the OPA627 for all amplifiers (A_{DC} = 120 dB, ω_{3dB} = 2π20 Hz), the absolute error of the impedance argument increases up to 28° for a measurement frequency of 1 MHz. It is mainly caused by

the amplifier A6 working with a gain of 10. When using the AD817 amplifier in this place with much greater bandwidth (A_{DC} = 5000, $\omega_{3dB} = 2\pi 10$ kHz,) the error of the impedance argument decreases down to 6°. But the small open-loop DC gain of the AD817 introduced a systematic relative error of the impedance modulus on the level of 0.2% in the frequency range up to 100 kHz, increasing up to 2% at 1 MHz.

As the result of performed simulations the OPA627 has been used in amplifiers A1÷A4 and the AD817 for A5÷A7.

3.2. Capacitance of the shielded cables

In the second analysis stage, the influence of capacitance (C_L) existing at the input of the current-to-voltage converter (A1) on the impedance measurement error was examined. The resultant value of this capacitance is mainly dependent on the capacitance of the shielded cable connecting terminal L of the measured impedance Z_x to the input of A1, but also on the input capacitances of amplifier A1 and voltage follower A4. The simulations were performed for range resistor R_R = 10 kΩ, R_o = 1 kΩ and C_H = 20 pF (capacitance of the shielded cable connected to terminal H). Exemplary results of calculation are presented in Fig. 4.

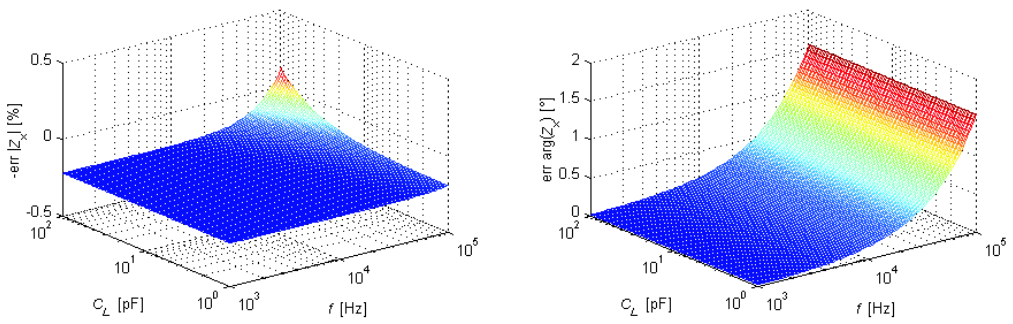

Fig. 4. Measurement error of modulus and argument of impedance of two-terminal RC network (R_x = 1 GΩ and C_x = 100 pF in parallel).

When analyzing graphs, it can be noticed that errors increase for frequencies above ca. 10 kHz. This is caused by the increase of the input impedance Z_{in} [8] of the current-to-voltage converter (A1). The increase of impedance Z_{in} causes an increase of the voltage on the resultant capacitance at the input of A1 and the virtual open-circuit between inputs "+" and "−" of amplifier A1 does not work properly.

Capacitance C_H of the second shielded cable connected to terminal H of impedance Z_x does not affect the measurement error (in simulation it was assumed that $C_H = C_L$). But it causes a decrease of the measurement signal applied to the impedance Z_x. In

order to eliminate this disadvantage, the analyzer allows to automatically correct the voltage across Z_x to keep it as programmed.

3.3. Parasitic capacitance C_R

In the third analysis stage, the influence of parasitic capacitance C_R shunting the range resistor has been examined. This capacitance results from the capacitance of range resistors, the capacitance entered by reed relays changing ranges and layout capacitances. Simulations were performed for a large value of range resistor $R_R = 100$ MΩ in order to emphasize difficult conditions for the current-to-voltage converter. Errors of impedance Z_x modulus and argument (Fig. 5) were calculated for the following values of $R_o = 10$ MΩ, $C_o = 2$ pF, $C_H = C_L = 20$ pF.

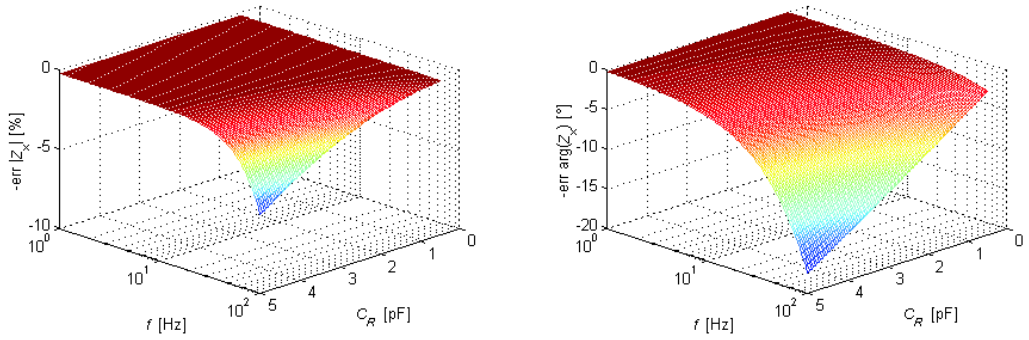

Fig. 5. Measurement error of modulus and argument of impedance as a function of parasitic capacitance C_R.

When analysing graphs, the significant influence of parasitic capacitance C_R on the error of impedance measurement for frequencies higher than 10 Hz can be noticed. The maximal frequency is also dependant on range resistor R_R. Because of this, the maximal frequency value increases for ranges with a smaller value of the range resistor. In the realised analyser there is the possibility of decreasing this error by using range impedance Z_R instead of range resistance R_R.

4. CORRECTION OF MEASUREMENT RESULTS

Equation (1) can be used to correctly calculate parameters of the measured impedance assuring the condition that signals u_i and u_u extracted in the measurement probe are dependent only on current through i_x and voltage across u_x impedance Z_x. The performed analysis shows that signals u_i and u_u depend also on unwanted parameters (e.g. layout capacitances, real-life parameters of operational amplifiers) causing impedance measurement errors. Because of this, there is the need to develop a corrected version

of formula (1) which will take into account real parameters of signals in the probe. To do this, an equivalent circuit of the probe was proposed and presented in Fig. 6. This circuit takes into account elements which decided on errors in the previously presented analysis.

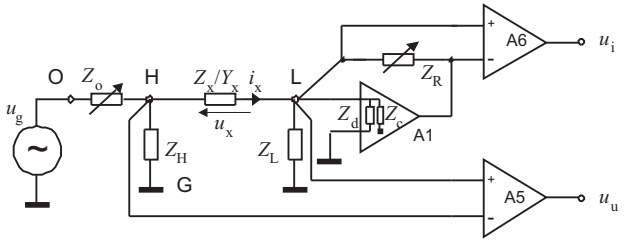

Fig. 6. Equivalent circuit of the probe.

On the basis of the equivalent circuit of the probe the equations describing signal u_i and u_u have been derived:

$$U_i = \frac{Z_R}{Z_x}\left\{\frac{\frac{10}{1+\frac{11}{A_u^{A6}}}}{1+\frac{1}{A_u^{A1}}\left[1+\frac{Z_R}{Z_x}+Z_R\left(\frac{1}{Z_d}+\frac{1}{Z_c}+\frac{1}{Z_L}\right)\right]}\right\}U_g, \tag{2}$$

where: $Z_R = \dfrac{1}{\frac{1}{R_R}+j\omega C_R}$ – the impedance consisting of the parallel connection of range resistor R_R and capacitance C_R, Z_d and Z_c – the differential and common input impedance of amplifier A1, Z_L – the impedance taking into account shielded-cable capacitance and input impedance of the voltage follower A4.

$A_u^{A1/6} = \dfrac{A_{DC}}{1+j\frac{\omega}{\omega_{3dB}}}$ – is the single-pole (ω_{3dB}) transfer function of amplifier A1 and A6, A_{DC} – open-loop DC gain of amplifiers.

$$U_u = \frac{Z_x}{Z_x+\frac{1}{\frac{1}{Z_{in}}+\frac{1}{Z_L}}}U_g, \tag{3}$$

where: $Z_{in} = \dfrac{1}{\frac{1}{Z_d}+\frac{1}{Z_c}+\frac{1+A_u}{Z_R}}$ – the input impedance of the current-to-voltage converter A1 [8].

Using (2) and (3) which take into account the influence of all unwanted sources of errors and results of simulation performed in Section 3, the formula for calculation of the measured impedance Z_m has been derived:

$$Z_m = \frac{U_u}{U_i} \frac{10Z_R}{1 + \frac{11}{A_u^{A6}}}. \tag{4}$$

Equation (4) takes into account the error sources which have the greatest influence: capacitance C_R and parameters of amplifier A6 with required gain equal to 10. Section 5 shows profits appearing from the use of (4) when calculating the modulus and argument of the measured impedance.

5. EXPERIMENTAL RESULTS AND DISCUSSION

In order to verify the proposed formula (4), a measurement using the realized probe and high impedance analyzer was performed. As the object under test, the reference two-terminal RC network shown in Fig. 7 was connected to the probe terminals.

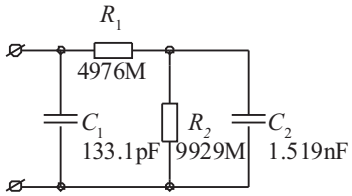

Fig. 7. Electrical schematic diagram of the reference two-terminal RC network.

The two-terminal network used for tests exemplifies a typical equivalent circuit of the impedance of an anticorrosion coating in its early stage of life. The capacitors of the two-terminal network were measured with a HP4192 impedance analyzer assuring an error not exceeding 0.1%, but resistors were measured by the technical method using a reference resistor of 10 MΩ ± 0.01% and a HP34401A multimeter.

Ten measurement series were performed for frequencies in range of 1 MHz÷1 mHz (with 1-2-5 step) with an AC signal of 1 V_{RMS} amplitude. Mean values were calculated for results of impedance modulus and argument measurement (on the basis of (1)) and they are presented in Fig. 8. For each measurement point (except 500 kHz and 1 MHz) the standard deviation of the impedance modulus does not exceed 0.15%, and for the argument it is less than 0.3°.

When comparing the obtained curves, small differences can only be observed for the impedance argument at high frequencies. In order to make a precise evaluation of the accuracy possible, the relative error of the impedance modulus and the absolute error of the impedance argument were calculated. They were determined using reference characteristics of the object resulting from values of the RC components presented in Fig. 7.

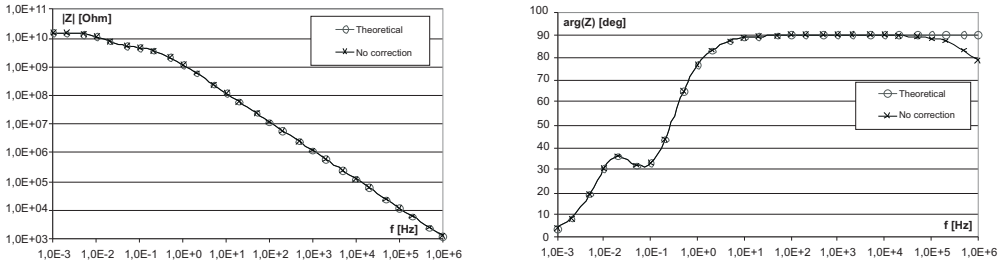

Fig. 8. Modulus and argument of impedance of a two-terminal RC network calculated theoretically and measured without correction.

Figure 9 presents also the errors of the impedance measurement which were obtained using formula (4) to calculate the modulus and argument of impedance on the basis of the same results of measurement of signals u_i and u_u extracted in the probe. When using (4) it was assumed that $C_R = 1$ pF (on the basis of the measurement capacitance of resistors R_R it is ca. 0.24 pF, and for 7 reed relays ca. 7×0.1 pF) and amplifier AD817 ($\omega_{3dB} = 2\pi 10$ kHz and $A_{DC} = 5000$) was used as A6 with the gain equal to 10. When analyzing the graphs it can be seen that the influence of the presented parameters is mostly important for frequencies above 100 kHz in case of the modulus and even above 20 kHz in case of the argument of the impedance. It is also seen that the impedance modulus error decreases (ca. 0.2%) in the whole frequency range due to the gain correction of amplifier A6 caused by the small open-loop DC gain of AD817 ($A_{DC} = 5000$).

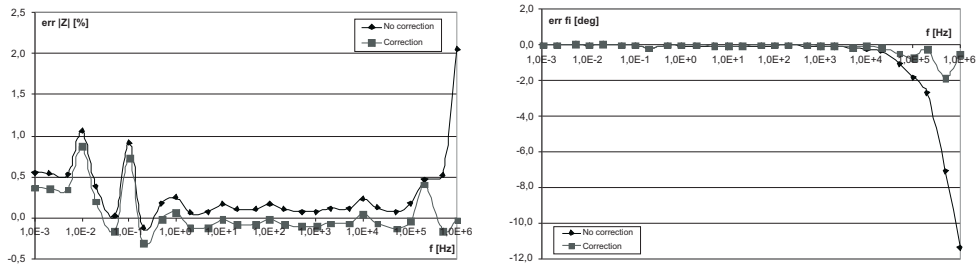

Fig. 9. Relative error of modulus and absolute error of argument of impedance of a two-terminal RC network without correction and taking into account the compensation of the parasitic capacitance C_R and parameters ω_{3dB} and A_{DC} of the operational amplifier.

The increase of the impedance modulus error in the frequency range of 0.01 Hz ÷ 0.2 Hz is caused by superposition of errors of determining the orthogonal parts of signals u_u and u_i with errors entered by the measurement probe. In this frequency range the orthogonal parts are comparable, so the error of their determination is greater. For frequencies above 1 Hz and below 0.01 Hz, the object has one dominating

part: imaginary or real, so they are determined with lower error and are almost unseen in Fig. 9.

Resuming, one can notice that the tests of a real-life measurement probe fully proved the presented analysis. It creates the possibility of using simulations in the development process of the probe in order to minimize measurement errors. The most important profit appearing from the performed analysis is the implementation of formula (4) in the realized analyzer. It allowed to increase the accuracy of measurements, especially in the high frequency region above 100 kHz.

6. CONCLUSIONS

The realized analyzer, thanks to the use of the input circuit in the form of a measurement probe can measure impedance in the range of 100 $\Omega < Z_m \leq 100$ GΩ (in 8 subranges). The use of the current-to-voltage converter allows elimination of the influence of the capacitance of shielded cables at the input of the probe on the error of impedance measurement. In order to determine the orthogonal parts of the measurement signals, the digital signal processing technique was employed in the analyzer. This makes it possible to measure in a wide frequency range starting from very low 100 μHz up to 1 MHz.

An analysis of the probe was performed to evaluate impedance measurement accuracy. Strong dependence was found of the error of impedance modulus and argument on parasitic capacitance existing in parallel to the range resistor and on parameters of the transfer function of amplifier with gain equal to 10 (in the high frequency range >100 kHz). Comparison of the simulation and measurement results of the realized probe proved that the assumed equivalent circuit correctly describes real-life parameters of the probe. Because of this, the formula describing the extracted signals can be used to develop the equation correcting the influence of the parasitic capacitances and real-life parameters of the operational amplifiers. It was shown that the parameters of the measured impedance can be determined with maximal 1% error in case of the impedance modulus in the whole frequency range and 0.5° in case of the impedance argument for frequencies up to 200 kHz and 2° for higher frequencies up to 1 MHz. The developed formula, meaningfully increasing the impedance measurement accuracy, was implemented in the software of the computer controlling the analyzer.

REFERENCES

1. Andersson H. et al.: *Modelling electrochemical impedance data for semi-bipolar lead acid batteries*. J. Applied Electrochemistry, vol. 31, no. 1, 2001, pp. –11.
2. Srinivas K. et al.: *Impedance spectroscopy study of polycrystalline* $BI_6FE_2TI_3O_{18}$. Bull. Mater. Sci. vol. 26 no. 2, 2003, pp. 247–253.
3. Xiang J. et al.: *Direct inversion of the apparent complex-resistivity spectrum*. Geophysics, vol. 66, no. 5, 2001, pp. 1399–1404.

4. Coverdale R.T. et al.: *Interpretation of impedance spectroscopy of cement paste via computer modeling.* Jour. Mat. Sci. vol. 30, 1995, pp. 712–719.
5. Nebuya S. et al.: *Measurement of high frequency electrical transfer impedances from biological tissues*. Electronics Lett., vol. 35, no. 23, 1999, pp. 1985–1987.
6. Carullo A. et al.: *Fast impedance analyzer for corrosion monitoring.* Proc. of XVI IMEKO World Congress, vol. 6, Vienna, 2000, pp. 161–166.
7. Hoja J., Lentka G.: *Virtual instrument using bilinear transformation for parameter identification of high impedance objects*, Meas. Sci. Tech., vol. 14, no. 5, 2003, pp. 633–642.
8. Franco S.: *Operational amplifiers and analog integrated circuits*. McGraw-Hill Book Company, 1988.